

ChemBioChem

Combining Chemistry and Biology



**Chemistry
Europe**

European Chemical
Societies Publishing



Reprint

WILEY-VCH

VIP Very Important Paper

Structural and Biochemical Insight into the Recruitment of Acyl Carrier Protein-Linked Extender Units in Ansamitocin Biosynthesis

Fa Zhang, Huining Ji, Imtiaz Ali, Zixin Deng, Linqun Bai, and Jianting Zheng*^[a]

A few acyltransferase (AT) domains of modular polyketide synthases (PKSs) recruit acyl carrier protein (ACP)-linked extender units with unusual C2 substituents to confer functionalities that are not available in coenzyme A (CoA)-linked ones. In this study, an AT specific for methoxymalonyl (MOM)-ACP in the third module of the ansamitocin PKS was structurally and biochemically characterized. The AT uses a conserved tryptophan residue at the entrance of the substrate binding tunnel to discriminate between different carriers. A W275R mutation switches its carrier specificity from the ACP to the CoA molecule. The acyl-AT complex structures clearly show that the MOM-ACP accepted by the AT has the 2S instead of the opposite 2R stereochemistry that is predicted according to the biosynthetic derivation from a D-glycolytic intermediate. Together, these results reveal the structural basis of ATs recognizing ACP-linked extender units in polyketide biosynthesis.

Complex polyketides are a large group of structurally diverse natural products with antibacterial, antifungal, antitumor, and anticholesterol properties. They are biosynthesized by modular polyketide synthases (PKSs) from simple carboxylic acids activated by either coenzyme A (CoA) or acyl carrier proteins (ACPs).^[1] An acyltransferase (AT) domain selects the extender unit to be incorporated into the growing polyketide backbone and therefore acts as the “gatekeeper” of each PKS module.^[2] AT-catalyzed transacylation reactions involve a ping-pong mechanism. In the first half of the reaction, the active site serine is esterified by an extender unit to form an acyl-AT intermediate. In the second step, the extender unit is transferred to the phosphopantetheine arm of the downstream ACP, along with the formation of a transient AT-ACP complex. Classical ATs selectively recruit CoA-linked extender units, such as malonyl-CoA (M-CoA), methylmalonyl-CoA (MM-CoA), and less frequently, ethylmalonyl-CoA (EM-CoA) to incorporate acetate, propionate, and butyrate, respectively. A small number of ATs use extender units biosynthesized on ACP carriers instead of CoA molecules to expand substrate repertory of modular PKSs and form highly specialized structures. Up to now, several ACP-linked extender units have been identified in polyketide bio-

synthetic pathways, including methoxymalonyl (MOM)-ACP, hydroxymalonyl (HM)-ACP, and aminomalonyl (AM)-ACP.^[3] During the elongation of polyketide intermediates, these ACP-linked extender units install unusual C2 substituents (methoxy, hydroxy, or amino) that are not available in acyl-CoAs. Compared with the CoA-specific ATs, the ATs specific for ACP-linked substrates involve additional protein-protein interactions in the first half of the transacylation reaction. The *trans*-acting AT, ZmaF, and the *cis*-acting AT, ZmaA-AT, recognizing AM-ACP and HM-ACP respectively in zwittermicin biosynthesis, have been extensively investigated.^[3a] The apo structure of ZmaA-AT specific for HM-ACP is solved to 1.7 Å.^[4] In vitro biochemical assays of ZmaF reveal remarkable acyl-promiscuity for ACP-linked extender units.^[5] However, the structural basis of these special ATs distinguishing between ACP and CoA carriers is still obscure. The potential ATs specific for ACP-linked substrates in polyketide diversification is relatively underexplored relative to the canonical CoA specific ATs.

Ansamitocin P-3 (AP-3; Figure 1) is a highly potent antitumor polyketide produced by *Actinosynnema pretiosum*.^[3c] Antibody conjugates of AP-3 are clinically used for treating breast cancers.^[3e] The AP-3 gene cluster has been cloned and the biosynthetic pathway was determined by isotopic feeding, in vivo

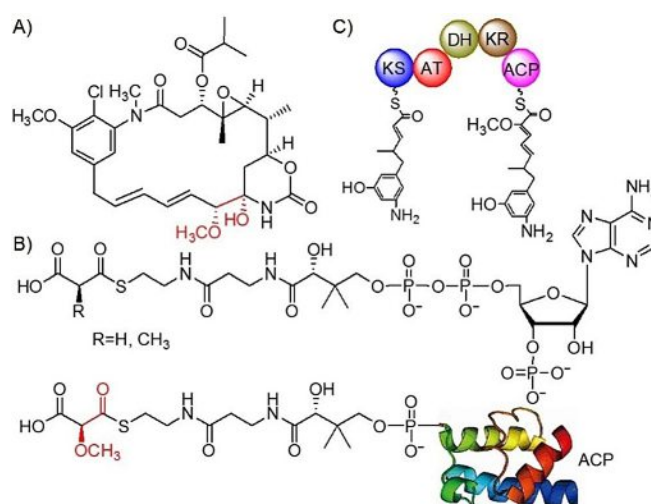


Figure 1. Biosynthesis of AP-3 involves a MOM-ACP extender unit. A) The chemical structure of AP3. The atoms derived from the MOM-ACP extender unit are in red. B) CoA- and ACP-linked extender units. The ACP is shown as cartoon. The serine carrying the phosphopantetheinyl is shown as sticks. C) The AT domain in the third module of AP-3 PKS selects the MOM-ACP extender unit.

[a] F. Zhang, H. Ji, I. Ali, Prof. Z. Deng, Prof. L. Bai, Prof. J. Zheng
State Key Laboratory of Microbial Metabolism
School of Life Sciences and Biotechnology, Shanghai Jiao Tong University
800 Dongchuan Road, Minhang District, 200240 Shanghai (P. R. China)
E-mail: jtzheng@sjtu.edu.cn

Supporting Information and the ORCID identification numbers for the authors of this article can be found under <https://doi.org/10.1002/cbic.201900628>.

gene inactivation, and in vitro enzymatic analysis experiments.^[6] Assembly of the 19-membered macrolactam of AP-3 involves a MOM-ACP extender unit. A subcluster of five genes (*asm13-17*) is involved in the biosynthesis of the MOM-ACP. A mutant with interrupted *asm15* shows no ansamitocin production, but produces small amounts of a 10-desmethoxy-ansamitocin derivative due to the incorporation of a M-CoA in the absence of the MOM-ACP. However, inactivation of *asm14* that encodes the discrete ACP carrier eliminates the production of any ansamitocin-related compounds.^[3c] The common glycolytic intermediate 1,3-bisphospho-D-glycerate is the precursor of the MOM-ACP extender unit. Due to the stereospecificity of the glycolytic pathway, the MOM-ACP is predicted to have *R* configuration at C2 (Figure S1 in the Supporting Information).^[3b] Thus, the (2*R*)-MOM-Asm14 is structurally and stereochemically distinct from the (2*S*)-acyl-CoA extender units that are selected by CoA-specific ATs.^[7] In AP-3 biosynthesis the AT of the third module of the AP-3 PKS (AsmAT3) is responsible for recognition of the MOM-Asm14 extender unit and loads the MOM onto the phosphopantetheinyl group of the downstream cognate AsmACP3 (Figure 1 B and C).^[6f] Interestingly, no obvious sequence signature could distinguish AsmAT3 from other ATs of modular PKSs. Herein, we report the crystal structures of the apo and acylated AsmAT3. The importance of a conserved tryptophan at the entrance of the substrate binding tunnel in discriminating between ACP and CoA carriers was revealed by structural comparisons of AsmAT3 with previously reported CoA specific ATs.^[7b,c] Mutation of the single tryptophan residue altered the carrier specificity of AsmAT3 from ACP to CoA. These results disclosed an important residue position involved in substrate recognition. Moreover, the 2*S* preference of AsmAT3 was revealed by acyl-AT complex structures and confirmed by biochemical assays, implying that an additional obligatory epimerization step is involved in MOM-Asm14 biosynthesis.

For in vitro functional assays, AsmAT3 including its N-terminal ketosynthase (KS)-AT linker was overexpressed as an isolated domain and purified to homogeneity.^[8] M-CoA, (2*RS*)-MM-CoA and (2*RS*)-MOM-CoA were used to evaluate the hydrolytic activity of AsmAT3 toward CoA-linked substrates by monitoring the thiol group of released CoA with Ellman's reagent.^[9] The corresponding malonate (obs. 103.0040, calcd 103.0037), methylmalonate (obs. 117.0189, calcd 117.0193) and methoxymalate (obs. 133.0138, calcd 133.0142) were confirmed by mass spectrometry (MS). Previous studies have suggested that the formation of the acyl-enzyme intermediate was the most important step in the substrate discrimination of AT domains.^[9,10] The hydrolytic rate of acyl-CoA catalyzed by an AT domain in the absence of a cognate holo-ACP may reflect its intrinsic substrate specificity. AsmAT3 is more than 700 times less active than canonical CoA-specific ATs (Table 1). M-CoA is more efficiently used by AsmAT3, consistent with the production of small amounts of 10-desmethoxy-ansamitocin in *asm15* disrupted strain. Asm14, the discrete ACP carrier, was expressed and purified as an apo protein. MOM-Asm14 was then enzymatically synthesized in vitro from (2*RS*)-MOM-CoA by using the promiscuous Sfp phosphopantetheinyl transferase

Table 1. Kinetic parameters of ATs.

ATs	Substrate ^[a]	$k_{\text{cat}}, K_{\text{M}}$ [mM ⁻¹ min ⁻¹]	k_{cat} [min ⁻¹]	K_{M} [mM]
AsmAT3	M-CoA	0.35 ± 0.049	0.41 ± 0.021	1.17 ± 0.15
	MM-CoA	0.21 ± 0.036	0.26 ± 0.017	1.26 ± 0.20
	MOM-CoA	0.13 ± 0.032	0.20 ± 0.020	1.54 ± 0.34
	M-	52.31 ± 4.45	2.72 ± 0.10	0.052 ± 0.0038
	Asm14C76S			
	MM-	39.35 ± 4.74	2.44 ± 0.15	0.062 ± 0.0069
	Asm14C76S			
	MOM-	102.14 ± 12.17	2.86 ± 0.14	0.028 ± 0.0029
	Asm14C76S			
AsmAT3W275R	M-CoA	203.33 ± 57.58	3.05 ± 0.62	0.015 ± 0.0030
	MM-CoA	109.62 ± 28.79	2.85 ± 0.54	0.026 ± 0.0050
	MOM-CoA	58.10 ± 8.24	2.44 ± 0.14	0.042 ± 0.0050
	M-	17.23 ± 2.14	2.24 ± 0.14	0.13 ± 0.014
	Asm14C76S			
	MM-	16.27 ± 2.32	1.79 ± 0.13	0.11 ± 0.014
	Asm14C76S			
	MOM-	22.82 ± 1.40	1.78 ± 0.047	0.078 ± 0.0043
Asm14C76S				
SalAT2	M-CoA	255.00 ± 78.67	3.57 ± 0.77	0.014 ± 0.0031
SalAT2R270W	M-CoA	7.23 ± 1.30	0.34 ± 0.023	0.047 ± 0.0078

[a] (2*RS*)-MOM-CoA and (2*RS*)-MM-CoA were used in kinetic assays and preparations of acyl-Asm14C76S.

from *Bacillus subtilis* (Figure S2). Ellman's reagent was also used to monitor the thiol group of the ACP phosphopantetheinyl arm released in the AsmAT3 catalyzed hydrolysis of MOM-Asm14. Cys76 of Asm14 was mutated to serine to decrease background reactions derived from protein SH groups. The catalytic efficiency of AsmAT3 for MOM-Asm14C76S similar to those of canonical CoA specific ATs (Table 1),^[9,10] highlighting the importance of the AT-ACP interaction for incorporating the MOM extender unit in ansamitocin biosynthesis. AsmAT3 was slightly less efficient for M-Asm14C76S and MM-Asm14C76S (Table 1). The decreased activity is likely due to the specificity of AsmAT3 for acyl groups, suggesting additional substrate recognition derived from the acyl binding pocket.

The purified AsmAT3 was crystallized and the structure was solved by molecular replacement using EryAT5 (PDB ID: 2HG4)^[8a] as a search model and refined to 1.79 Å resolution (Table S1). Its overall fold closely resembles those of CoA specific ATs (PDB ID: 2QO3, 1.0 Å RMSD; PDB ID: 2HG4, 0.7 Å RMSD; PDB ID: 6IYO, 1.9 Å RMSD; PDB ID: 6IYR, 1.4 Å RMSD; PDB ID: 6IYT, 1.0 Å RMSD; PDB ID: 5YDA, 2.1 Å RMSD; PDB ID: 2G2Z, 2.2 Å RMSD; PDB ID: 4AMP, 3.5 Å RMSD)^[7b,8,10a,11] and that of ZmaAT (PDB ID: 4QBU, RMSD: 2.5 Å)^[4] recruiting HM-ACP. The AsmAT3 structure contains a KS-AT linker, an α/β -hydrolase subdomain and a ferredoxin-like subdomain (Figure 2).

The transacylation reaction performed by PKS ATs has been proposed to occur by a two-step ping-pong catalytic mechanism.^[2,9] If the serine-histidine catalytic dyad functions as in related ATs, S180 acts as a nucleophile to attack the thioester bond of the acyl donor to form a covalent acyl-O-ester inter-

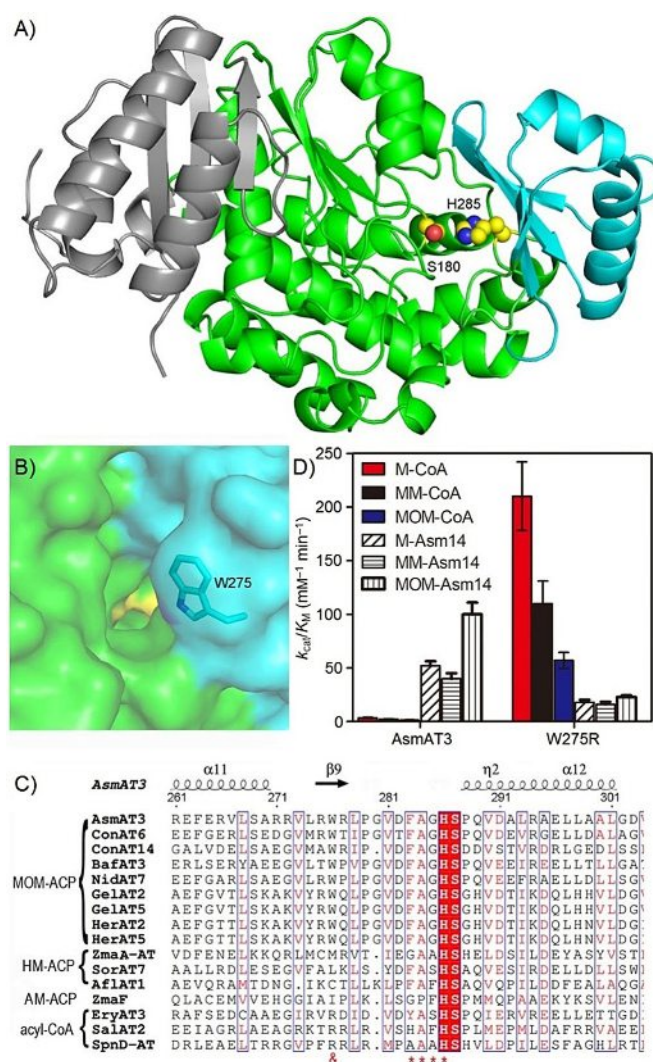


Figure 2. AsmAT3 uses a conserved tryptophan at the entrance of the substrate binding tunnel to discriminate between ACP and CoA carriers. A) The structure of AsmAT3 contains a KS-AT linker (gray), an α/β -hydrolase subdomain (green) and a ferredoxin-like subdomain (cyan). The catalytic serine and histidine are shown as spheres. B) The surface of AsmAT3 shows the entrance of the substrate binding tunnel of AsmAT3. The conserved tryptophan is shown as sticks. The structure is colored as in panel A. C) Sequence alignment of ATs selecting ACP- and CoA-linked extender units. The residue involved in carrier discrimination is labeled with “&”. The motif related to acyl group recognition is labeled with “*”. D) k_{cat}/K_M values of the AsmAT3 and its W275R mutant. AsmAT3 exhibits approximate 300-fold preference for MOM-Asm14 over cellular CoA-linked extender units. The W275R mutant shows decreased activity for Asm14 linked extender units but significantly increased activity for CoA linked extender units. MOM-ACP, methoxymalonyl-ACP; HM-ACP, hydroxymalonyl-ACP; AM-ACP, aminomalonyl-ACP. AsmAT3: module 3 of ansmotisin PKS; ConAT6: module 6 of concanamycin PKS; ConAT14: module 14 of concanamycin PKS; BafAT3: module 3 of bafilomycin PKS; NidAT7: module 7 of niddamycin PKS; GelAT2: module 2 of geldanamycin PKS; GelAT5: module 5 of geldanamycin PKS; HerAT2: module 2 of herbimycin PKS; HerAT5: module 5 of herbimycin PKS; Zma-AT: module 2 of zwittermixin A PKS; SorAT7: module 7 of soraphen PKS; AflAT1: module 1 of aflastatin PKS; ZmaF-AT: *trans* AT of zwittermixin A PKS; EryAT3: module 3 of erythromycin PKS; SalAT2: module 2 of salinomycin PKS; SpnD-AT: module 3 of splenocin PKS.

mediate while H285 enhances the nucleophilicity of S180 by the deprotonation of the hydroxy group. A hydrogen bond is

formed between the side chain hydroxy group of the catalytic serine and the imidazole of the catalytic histidine in previously reported PKS AT structures.^[7b,8,10a,11] Interestingly, the side chain hydroxy group of the catalytic S180 forms a hydrogen bond with the imidazole of H179 instead of that of the catalytic H285 (Figure S3). This usual hydrogen bond between S180 and H179 is observed in MD simulations of AT5 models of monensin PKS with the MM-CoA or EM-CoA substrates.^[12] Previous studies suggest the conserved histidine in the GHSxG motif containing catalytic serine helps to decrease the hydrolysis rate by protecting acyl-AT intermediates.^[13] To disclose the structural basis of ATs discriminating between ACP- and CoA-linked substrates, AsmAT3 was compared with previously reported CoA specific ATs. The most obvious structural difference is that the active site entrance of AsmAT3 is constricted by the bulky side chain of W275 (Figure 2B and C). The corresponding position is occupied by an arginine in CoA specific ATs and by a hydrophobic methionine in ATs specific for HM-ACP and AM-ACP (Figure S4). W275 is located on the final β -strand of the ferredoxin-like subdomain of the AT. This region of an AT has been implicated in carrier recognition of extender units previously.^[4] A W275R mutant of AsmAT3 was engineered and its activity toward CoA- and ACP-linked substrates was evaluated by monitoring the released thiol group (Figure 2D and Table 1). The W275R mutant exhibits decreased activity toward acyl-Asm14 as measured by the k_{cat}/K_M values. However, it is almost as efficient as the canonical CoA specific ATs toward M-CoA and MM-CoA. The activity of the W275R mutant toward MOM-CoA is similar to that of the wild type AsmAT3 for MOM-ACP. The corresponding arginine of SalAT2 specific for M-CoA was mutated to tryptophan to further confirm functionality of the arginine in recognizing CoA. The activity of the resulting R270W mutant decreases 35 times toward the M-CoA extender unit. Interestingly, the single W to R mutation changes not only the carrier specificity but also the preference of the extender unit from MOM to M. The specificity for malonate as extender unit is likely overridden by the preference of ACP as carrier. We have analyzed the binding of M-CoA in SalAT2 substrate binding tunnel using molecular dynamics (MD) simulations previously.^[10a] Reinspection of the MD trajectories reveals that the positively charged R270 interacts with the negatively charged diphosphate group of CoA (Figure S5). The tryptophan/arginine motif is relatively conserved, suggesting that ATs of modular PKSs may use a similar strategy to discriminate between ACP- and CoA-linked substrates (Figure S11).

The *S* preference of CoA-specific ATs has been confirmed by biochemical assays of erythromycin PKSs.^[7a] Although the C2 carbon of the MOM-ACP is predicted to have the opposite *2R* conformation in keeping with the biosynthetic derivation from the *D*-glycolytic intermediate, the catalytic residues of AsmAT3 are oriented as observed in ATs specific for (2*S*)-MM-CoA and (2*S*)-EM-CoA (Figure S3).^[7b,c,8,10a] To understand the substrate binding mode in the AsmAT3 active site, (2*RS*)-MOM-SNAC (*N*-acetyl cysteamine, “*S*” indicates the thioester linkage) was used as a substrate mimic in soaking experiments. A covalent intermediate structure with the MOM group attached to S180 was successfully obtained and refined to 1.77 Å resolution (Table S1

and Figure S6). This complex structure clearly shows that the 2S isomer of the racemic MOM-SNAC is selected by AsmAT3 (Figure 3). To assay the stereospecificity of AsmAT3, (2R)-MOM-SNAC was enzymatically synthesized by a promiscuous acyl-CoA ligase, *Streptomyces coelicolor* MatB (Figures 3B, C and S7).^[14] AsmAT3 did not show any activity toward the SNAC-linked 2R substrate. However, when the *S. coelicolor* MM-CoA epimerase was supplemented in the reactions, the release of SNAC was observed (Figure 3B), suggesting the 2S epimer could be hydrolyzed by AsmAT3. (2R)-MOM-CoA and (2R)-MM-CoA were also enzymatically synthesized to further confirm the

2S stereospecificity of AsmAT3 (Figure S7). The W275R mutant was used due to its high activity toward CoA-linked substrates. In both cases, the release of free SH was only observed in the presence of MM-CoA epimerase (Figure S8). Next, Sfp was used to enzymatically synthesize (2R)-MOM-Asm14 from apo-Asm14 and (2R)-MOM-CoA to assay the stereoselectivity of AsmAT3 in the presence of the cognate holo-AsmACP3 cosubstrate. As expected, the (2R)-MOM-AsmACP3 was not detected by mass spectrometry. However, when (2RS)-MOM-Asm14 derived from (2RS)-MOM-CoA served as the acyl donor, the MOM-AsmACP3 was observed (Figure S9), reaffirming the 2S stereospecificity of AsmAT3 in transacylation reactions. Because the common glycolytic intermediate 1,3-bisphospho-D-glycerate is the metabolic origin of the MOM-ACP extender unit, an additional obligatory epimerization step is required to convert the configuration of C2 from R to S. ZmaA-AT specific for HM-ACP may also stereospecifically recognize the 2S isomer considering its structural similarity to AsmAT3. An FAD-dependent oxidation step in HM-ACP biosynthesis has been proposed to proceed via an enediol intermediate to form the 2S stereoisomer.^[4]

In the MOM-AsmAT3 complex structure, the side chain of catalytic S180 rotates about 97° relative to the apo structure and adopts the orientation observed in previously reported ATs (Figure S3), consistent with the role of H285 as a general base to deprotonate S180 for nucleophilic attack on the carbonyl carbon of the substrate. In the FabD^[11b] and SpnD-AT^[7b] complex structures, the guanidino group of the conserved arginine at the bottom of the acyl binding pocket stabilizes the C3 carboxyl group of the acylated malonate derivative through a bidentate salt bridge (Figure S10A). In the MOM-AsmAT3 complex structure, both the C3 carboxylate group and the conserved R205 are differently oriented. The C3 carboxylate group of MOM adopts a vertical orientation with respect to that of malonyl observed in FabD and SpnD-AT complex structures (Figure S10A) while the guanidino group of the R205 of MOM-AsmAT3 rotates about 60° relative to the corresponding arginine of FabD and SpnD-AT (Figure S10A). The R205 of apo structure adopts the same orientation as observed in the complex structure. The side chain of N332 forms a hydrogen bond with R205 and likely helps to position the guanidino group (Figure S10B). The unusual orientation of the conserved arginine is also observed in the apo structure of EryAT3 specific for MM-CoA and SalAT14 specific for EM-CoA. Moreover, two water molecules and the Q152 side chain are involved in the stabilization of the C3 carboxylate of the acylated MOM. The Q98 and Q181 may help to stabilize the substrate carbonyl during the reaction (Figure S10C).^[15] Consequently, these two residues are more ordered in the complex structure than in the apo structure. As observed in SpnD-AT complex structures, these multiple hydrogen bonds help the enzyme to selectively bind the S-stereoisomer with the C2 substituent surrounded by M219, L277, Q98, Q152, V280, F282, and H285 (Figure S10D). The C2 substituent in an R-orientation would sterically clash with the catalytic histidine. The ¹⁷⁸GHSXG¹⁸² motif centered on the active site serine and the ²⁸²FAGH²⁸⁵ motif containing the catalytic histidine have been correlated to acyl-specificity of ATs (Figures S11 and 2C). The X following the catalyt-

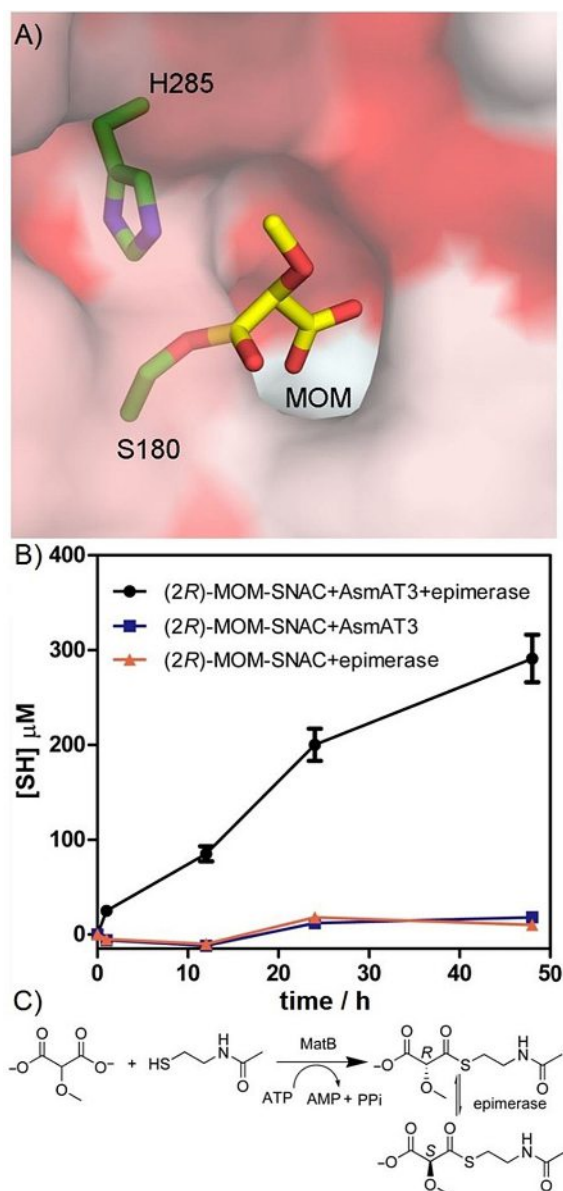


Figure 3. The stereochemistry of AsmAT3. A) The MOM-AT complex structure clearly shows the S-configuration preference of AsmAT3. The catalytic serine, catalytic histidine, and MOM are shown as sticks. The surface is shown as a gradient from hydrophobic (red) to hydrophilic (white). B) Release of the SNAC thiol. The enzyme shows no activity toward the (2R)-MOM-SNAC. The release of SNAC is observed in reactions containing MM-CoA epimerase. C) MatB enzymatically catalyzes the synthesis of (2R)-MOM-SNAC. The *S. coelicolor* MM-CoA epimerase converts (2R)-MOM-SNAC into (2S)-MOM-SNAC.

ic serine in the GHSXG motif is a glutamine in AsmAT3 and other MOM-ACP specific ATs, like MM-CoA specific ATs. The side chain of the Q181 forms a hydrogen bond with the Q98 contacting the substrate carbonyl in the complex structure (Figure S10C). The X is usually a bulky branched hydrophobic amino acid in M-CoA specific ATs. The ²⁸²FAGH²⁸⁵ of AsmAT3 is distinct from the M-CoA specific HAFH motif and the MM-CoA specific YASH motif. Like the *trans*-acting ZmaF recognizing AM-ACP, AsmAT3 shows promiscuity toward acyl groups of the extender units, suggesting the protein interaction between carrier ACP and AT plays a major role in substrate recognition.

Trapping Acyl-AT complex structures are challenging due to the rapid hydrolysis of the intermediates.^[10a] A glycerol molecule was observed at the entrance of the substrate binding tunnel of AsmAT3 (Figure S12) and may help to stabilize the acyl-AT intermediate by preventing it from water molecules. MM-CoA is the most widely used extender unit in polyketide biosynthesis. The efforts to switch the specificity of an AT from MM-CoA to an alternative extender unit are hampered by the lack of the MM-AT complex structure.^[16] Therefore, MM-CoA was used in soaking experiments to decipher its binding mode in AsmAT3. The resulting MM-AsmAT3 complex structure was solved to 1.83 Å resolution. The binding mode of the MM group is very similar to that of the MOM group observed in the MOM-AsmAT3 complex structure. No obvious structural changes were observed (Figure S13B). Considering the structural similarity of PKS ATs, the binding mode of MM in AsmAT3 may represent that in the active site of canonical MM-CoA specific ATs.

Extender units biosynthesized on ACP carriers instead of CoA molecules are of interest in engineering of polyketides. The substituents introduced by ACP-linked extender units serve critical functions within the product and can be potentially used in downstream semi-synthetic derivatizations. To selectively recruit these rare extender units, ATs in PKS modules must exclude abundant cellular malonyl-CoA derivatives. Kinetic analysis revealed an approximate 300-fold preference of MOM-Asm14 over cellular CoA-linked extender units. Structural and biochemical assays of AsmAT3 showed that a tryptophan/arginine motif located at the entrance of the substrate binding tunnel was responsible for discriminating between ACP and CoA carrier molecules. Moreover, we presented both structural and biochemical evidence to support the preference of AsmAT3 for the 2*S* stereoisomer over the 2*R* stereoisomer in the incorporation of MOM-Asm14 and excluded the speculation of an unusual AT recognizing (2*R*)-MOM-ACP extender unit in AP-3 biosynthesis.^[1,3b] These results represent important steps toward understanding the incorporation of unusual ACP-linked extender units in assembly of polyketide backbones.

Acknowledgements

We thank the staff of beamline BL18U1 at the National Center for Protein Science Shanghai (China) for access and help with X-ray data collection. We also thank Dr. Lei Feng of the Instrumen-

tal Analysis Center of Shanghai Jiao Tong University for her kind help with LC-MS analysis. This work was supported by the National Natural Science Foundation of China (31570056 and 31770068).

Conflict of Interest

The authors declare no conflict of interest.

Keywords: acyltransferase · biosynthesis · carrier specificity · extender units · polyketides

- [1] Y. A. Chan, A. M. Podevels, B. M. Kevany, M. G. Thomas, *Nat. Prod. Rep.* **2009**, *26*, 90–114.
- [2] B. J. Dunn, C. Khosla, *J. R. Soc. Interface* **2013**, *10*, 20130297.
- [3] a) Y. A. Chan, M. G. Thomas, *Biochemistry* **2010**, *49*, 3667–3677; b) S. C. Wenzel, R. M. Williamson, C. Grunanger, J. Xu, K. Gerth, R. A. Martinez, S. J. Moss, B. J. Carroll, S. Grond, C. J. Unkefer, R. Muller, H. G. Floss, *J. Am. Chem. Soc.* **2006**, *128*, 14325–14336; c) B. J. Carroll, S. J. Moss, L. Bai, Y. Kato, S. Toelzer, T. W. Yu, H. G. Floss, *J. Am. Chem. Soc.* **2002**, *124*, 4176–4177; d) Y. A. Chan, M. T. Boyne, A. M. Podevels, A. K. Klimowicz, J. Handelsman, N. L. Kelleher, M. G. Thomas, *Proc. Natl. Acad. Sci. USA* **2006**, *103*, 14349–14354; e) L. Amiri-Kordestani, G. M. Blumenthal, Q. C. Xu, L. Zhang, S. W. Tang, L. Ha, W. C. Weinberg, B. Chi, R. Candau-Chacon, P. Hughes, A. M. Russell, S. P. Miksinski, X. H. Chen, W. D. McGuinn, T. Palmby, S. J. Schrieber, Q. Liu, J. Wang, P. Song, N. Mehrotra, L. Skarupa, K. Clouse, A. Al-Hakim, R. Sridhara, A. Ibrahim, R. Justice, R. Pazdur, *Clin. Cancer Res.* **2014**, *20*, 4436–4441.
- [4] H. Park, B. M. Kevany, D. H. Dyer, M. G. Thomas, K. T. Forest, *PLoS One* **2014**, *9*, e110965.
- [5] S. M. Carpenter, G. J. Williams, *ACS Chem. Biol.* **2018**, *13*, 3361–3373.
- [6] a) X. Ning, X. Wang, Y. Wu, Q. Kang, L. Bai, *Biotechnol. J.* **2017**, *12*, 1700484; b) Y. Kato, L. Bai, Q. Xue, W. P. Revill, T. W. Yu, H. G. Floss, *J. Am. Chem. Soc.* **2002**, *124*, 5268–5269; c) S. J. Moss, L. Bai, S. Toelzer, B. J. Carroll, T. Mahmud, T. W. Yu, H. G. Floss, *J. Am. Chem. Soc.* **2002**, *124*, 6544–6545; d) P. Spitteller, L. Bai, G. Shang, B. J. Carroll, T. W. Yu, H. G. Floss, *J. Am. Chem. Soc.* **2003**, *125*, 14236–14237; e) F. Taft, M. Brunjes, T. Knobloch, H. G. Floss, A. Kirschning, *J. Am. Chem. Soc.* **2009**, *131*, 3812–3813; f) T. W. Yu, L. Bai, D. Clade, D. Hoffmann, S. Toelzer, K. Q. Trinh, J. Xu, S. J. Moss, E. Leistner, H. G. Floss, *Proc. Natl. Acad. Sci. USA* **2002**, *99*, 7968–7973.
- [7] a) A. F. Marsden, P. Caffrey, J. F. Aparicio, M. S. Loughran, J. Staunton, P. F. Leadlay, *Science* **1994**, *263*, 378–380; b) Y. Li, W. Zhang, H. Zhang, W. Tian, L. Wu, S. Wang, M. Zheng, J. Zhang, C. Sun, Z. Deng, Y. Sun, X. Qu, J. Zhou, *Angew. Chem. Int. Ed.* **2018**, *57*, 5823–5827; *Angew. Chem.* **2018**, *130*, 5925–5929; c) F. Wang, Y. Wang, J. Ji, Z. Zhou, J. Yu, H. Zhu, Z. Su, L. Zhang, J. Zheng, *ACS Chem. Biol.* **2015**, *10*, 1017–1025.
- [8] a) Y. Tang, C. Y. Kim, Mathews, II, D. E. Cane, C. Khosla, *Proc. Natl. Acad. Sci. USA* **2006**, *103*, 11124–11129; b) Y. Tang, A. Y. Chen, C. Y. Kim, D. E. Cane, C. Khosla, *Chem. Biol.* **2007**, *14*, 931–943.
- [9] B. J. Dunn, D. E. Cane, C. Khosla, *Biochemistry* **2013**, *52*, 1839–1841.
- [10] a) F. Zhang, T. Shi, H. Ji, I. Ali, S. Huang, Z. Deng, Q. Min, L. Bai, Y. L. Zhao, J. Zheng, *Biochemistry* **2019**, *58*, 2978–2986; b) B. J. Dunn, K. R. Watts, T. Robbins, D. E. Cane, C. Khosla, *Biochemistry* **2014**, *53*, 3796–3806.
- [11] a) C. W. Liew, M. Nilsson, M. W. Chen, H. Sun, T. Cornvik, Z. X. Liang, J. Lescar, *J. Biol. Chem.* **2012**, *287*, 23203–23215; b) C. Oefner, H. Schulz, A. D'Arcy, G. E. Dale, *Acta Crystallogr. Sect. D Biol. Crystallogr.* **2006**, *62*, 613–618.
- [12] K. Bravo-Rodriguez, A. F. Ismail-Ali, S. Klopries, S. Kushnir, S. Ismail, E. K. Fansa, A. Wittinghofer, F. Schulz, E. Sanchez-Garcia, *ChemBioChem* **2014**, *15*, 1991–1997.
- [13] S. Poust, I. Yoon, P. D. Adams, L. Katz, C. J. Petzold, J. D. Keasling, *PLoS One* **2014**, *9*, e109421.
- [14] A. J. Hughes, A. Keatinge-Clay, *Chem. Biol.* **2011**, *18*, 165–176.
- [15] P. Paiva, S. F. Sousa, M. J. Ramos, P. A. Fernandes, *ACS Catal.* **2018**, *8*, 4860–4872.

- [16] a) K. Bravo-Rodriguez, S. Klopries, K. R. Koopmans, U. Sundermann, S. Yahiaoui, J. Arens, E. Sanchez-Garcia, *Chem. Biol.* **2015**, *22*, 1425–1430; Version of record online: January 10, 2020
b) U. Sundermann, K. Bravo-Rodriguez, S. Klopries, S. Kushnir, H. Gomez, E. Sanchez-Garcia, F. Schulz, *ACS Chem. Biol.* **2013**, *8*, 443–450.
-

Manuscript received: October 15, 2019

Accepted manuscript online: November 27, 2019
